Article

Same-Single-Cell Analysis for the Study of Drug Efflux Modulation of Multidrug Resistant Cells Using a Microfluidic Chip

XiuJun Li, Victor Ling, and Paul C. H. Li

Anal. Chem., **2008**, 80 (11), 4095-4102 • DOI: 10.1021/ac800231k • Publication Date (Web): 30 April 2008

Anal. Chem. **2008,** *80,* 4095–4102

Same-Single-Cell Analysis for the Study of Drug Efflux Modulation of Multidrug Resistant Cells Using a Microfluidic Chip

XiuJun Li,[†] Victor Ling,[‡] and Paul C. H. Li*,[†]

Department of Chemistry, Simon Fraser University, Burnaby, BC, V5A 1S6, Canada, and BC Cancer Research Center, 675 West 10th Avenue, Vancouver, BC, V5Z 1L3, Canada

Since multidrug resistance (MDR) is a major cause of failure in cancer chemotherapy, we report a microfluidic approach combined with the same-single-cell analysis to investigate the modulation of MDR, manifested as the inhibition of drug efflux. A microfluidic chip that was capable of selecting and retaining a single multidrug-resistant cancer cell was used to investigate drug efflux inhibition in leukemia cell lines. Three advantages of the microfluidic-based same-single-cell analysis (dubbed as SASCA) method have been revealed. First, it readily detects the modulation of drug efflux of anticancer compounds (e.g., daunorubicin) by MDR modulators (e.g., verapamil) among cellular variations. Second, SASCA is able to compare the different cellular abilities in response to drug efflux modulation based on the drug transport kinetics of single cells. Third, SASCA requires only a small number of cells, which may be beneficial for investigating drug resistance in minor cell subpopulations (e.g., cancer "stem" cells).

Cancer chemotherapy has been impeded by the multidrug resistance (MDR) developed in cancer patients who are resistant to a variety of structurally unrelated cytotoxic drugs.[1–3] Tumors cells carrying the MDR phenotype are often associated with the overexpression of drug efflux pumps, among which the membrane-bound energy-dependent P-glycoprotein (Pgp) is one of the important classes. The Pgp efflux pump, which belongs to the superfamily of ATP binding cassette (ABC) transporters (i.e., ABCB1)[4] and is encoded by the MDR1 class of genes,[5] actively transports drugs out of the cancer cells. This has caused the intracellular drug concentration to be lower than the drug's cytotoxic threshold within cancer cells,[1] leading to the failure of many forms of chemotherapy.[4] Research advances in MDR have been summarized in several reviews.[4,6,7]

To improve chemotherapy sensitivity, Pgp inhibitors or MDR modulators are employed, and their effects on MDR reversal have been studied.[8–12] For instance, Ren et al. studied the efflux of doxorubicin in human carcinoma cells by a fluorescence plate reader, but not at the single-cell level.[8] Wang et al. developed a flow cytometry method to quantitatively assess Pgp inhibitors using daunorubicin as the drug and sodium vanadate as a positive control of MDR modulators.[9] While flow cytometry is a widely used technique to study MDR modulation, it does not provide the time-dependent drug transport kinetics of an individual single cell. Besides, flow cytometry typically requires 100,000 cells in the starting population to achieve reliable results.[13] This requirement is challenging when only a limited amount of hard-to-obtain cells (e.g., patient cancer cells) is available.

Recently, the microfluidic on-chip analysis has been applied to various biological systems. Since the small dimensions of microfluidic channels are compatible with the cell sizes, this has made the cell-based assay a popular micro total analysis system (μTAS) application since 2002.[14] The applications include cell culture,[15] cell trap and retention,[16–19] cell transport,[20] PCR,[21] FACS-on-a-chip,[13] patch clamp,[22] cell stimulation,[23] muscle cell

* Corresponding author. E-mail: paulli@sfu.ca. Phone: 778-782-5956. Fax: 778-782-3765.

† Simon Fraser University.

‡ BC Cancer Research Center.

(1) Marthinet, E.; Divita, G.; Bernaud, J.; Rigal, D.; Baggetto, L. G. *Gene Ther.* **2000**, *7*, 1224–1233.
(2) Persidis, A. *Nat. Biotechnol.* **1999**, *17*, 94–95.
(3) Locke, V. L.; Davey, R. A.; Davey, M. W. *Anti-Cancer Drugs* **2003**, *14*, 523–531.
(4) Higgins, C. F. *Nature* **2007**, *446*, 749–757.
(5) Gros, P.; Ben Neriah, Y. B.; Croop, J. M.; Housman, D. E. *Nature* **1986**, *323*, 728–731.
(6) Murthy, R. S. R.; Shah, N. M. *J. Biomed. Nanotech.* **2007**, *3*, 1–17.
(7) Dean, M.; Fojo, T.; Bates, S. *Nat. Rev. Cancer* **2005**, *5*, 275–284.
(8) Ren, Y.; Wei, D. *J. Pharm. Biomed. Anal.* **2004**, *36*, 387–391.
(9) Wang, E. J.; Casciano, C. N.; Clement, R. P.; Johnson, W. W. *Drug Metab. Dispos.* **2000**, *28*, 522–528.
(10) Efferth, T.; Davey, M.; Olbrich, A.; Rücker, G.; Gebhart, E.; Davey, R. *Blood Cells Mol. Dis.* **2002**, *28*, 160–168.
(11) Medeiros, B. C.; Landau, H. J.; Morrow, M.; Lockerbie, R. O.; Pitts, T.; Eckhardt, S. G. *Leukemia* **2007**, *21*, 739–746.
(12) Meaden, E. R.; Hoggard, P. G.; Khoo, S. H.; Back, D. J. *J. Immunol. Methods* **2002**, *262*, 159–165.
(13) Wang, M. M.; Tu, E.; Raymond, D. E.; Yang, J. M.; Zhang, H.; Hagen, N.; Dees, B.; Mercer, E. M.; Forster, A. H.; Kariv, I.; Marchand, P. J.; Butler, W. F. *Nat. Biotechnol.* **2005**, *23*, 83–87.
(14) Dittrich, P. S.; Tachikawa, K.; Manz, A. *Anal. Chem.* **2006**, *78*, 3887–3908.
(15) Gu, W.; Zhu, X. Y.; Futai, N.; Cho, B. S.; Takayama, S. *Proc. Natl. Acad. Sci. U.S.A.* **2004**, *101*, 15861–15866.
(16) Carlo, D. D.; Aghdam, N.; Lee, L. P. *Anal. Chem.* **2006**, *78*, 4925–4930.
(17) Li, X.; Li, P. C. H. *Anal. Chem.* **2005**, *77*, 4315–4322.
(18) Li, X.; Huang, J.; Tibbits, G. F.; Li, P. C. H. *Electrophoresis* **2007**, *28*, 4723–4733.
(19) Forry, S. P.; Reyes, D. R.; Gaitan, M.; Locascio, L. E. *J. Am. Chem. Soc.* **2006**, *128*, 13678–13679.
(20) Li, P. C. H.; Harrison, D. J. *Anal. Chem.* **1997**, *69*, 1564–1568.
(21) Kopp, M. U.; De Mello, A. J.; Manz, A. *Science* **1998**, *280*, 1046–1048.
(22) Chen, C.; Folch, A. *Lab Chip* **2006**, *6*, 1338–1345.

10.1021/ac800231k CCC: $40.75
Published on Web 04/30/2008

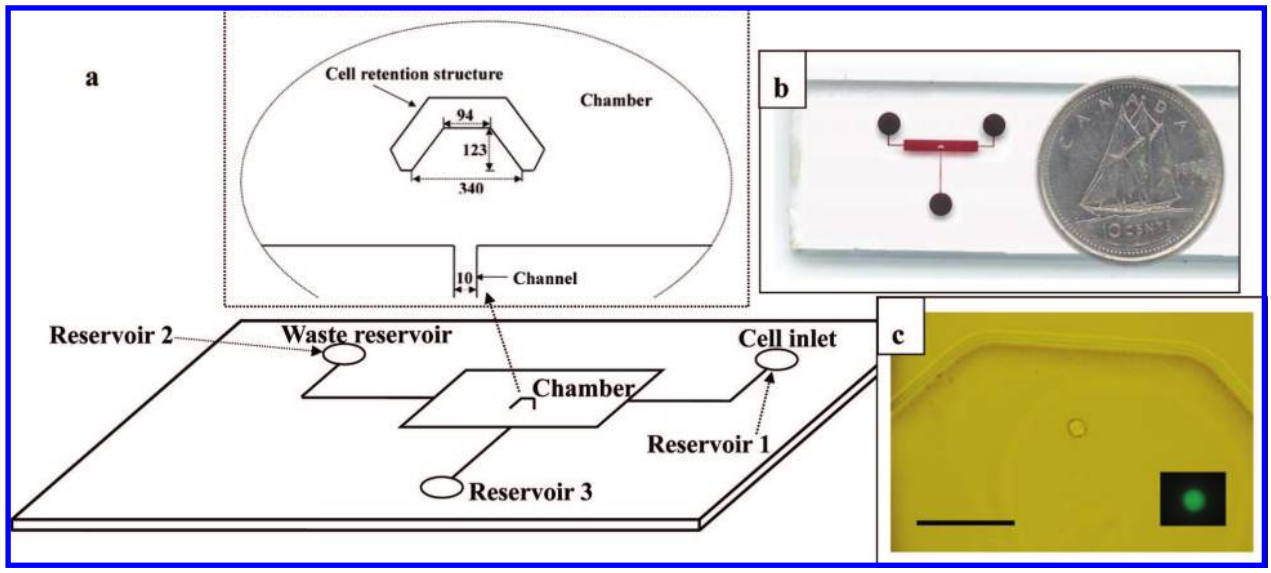

Figure 1. Layout of the microfluidic chip. (a) The schematics of the microfluidic chip consisting of 3 solution reservoirs and a cell retention structure, with the dimensions (in μm) shown in the inset. (b) An image of the microchip filled with a red food dye. A Canadian dime (10 cents) was placed on the chip for size comparison. (c) An image of a retained live single CEM/VLB cell, as stained by fluorescein diacetate (25 μM). The scale bar is 50 μm.

contraction and drug effect,[17,18] malaria-infected erythrocytes,[24] and so on. However, to date, no microfluidic studies on cancer cell MDR have been reported.

Among the microfluidic-based cellular applications, much emphasis has been placed on single-cell analysis recently.[25,26] Single-cell analysis is preferred because the traditional bulk cellular analysis often overlooks cellular heterogeneity and does not provide information on cell-to-cell variations (e.g., pattern of cellular response to a given stimulus,[27,28] or variability in the concentration of second messengers or metabolites among different cells[29–31]). When measuring the single-cell response on drugs or other stimuli in the microfluidic chip, a comparison (or control experiment) is usually needed. One common approach is based on the measurement from different single cells (denoted as the different-single-cell analysis or DISCA).[16,23,28,32] For instance, Carlo et al. studied the inhibition of intracellular carboxylesterases of HeLa cells based on the cellular responses from ~10 different cells at each concentration of the inhibitor compound.[16] Our group previously reported the degradation of IκB-EGFP (an inhibitory protein) in Jurkat cells by measuring the responses of 3 cells stimulated by TNF-α and another 3 cells untreated with the cytokine (control experiment).[32] We further studied the ionomycin-stimulated intracellular calcium $[Ca^{2+}]_i$ flux of 3 cardiomyocytes at 3 different concentrations of ionomycin.[17] Wheeler et al. investigated Fc$_\gamma$R-mediated $[Ca^{2+}]_i$ flux on three different U397 cells with one cell perfused with antibodies, and the other two cells as the control.[28]

In all the microfluidic studies to date, although cellular variations were observed, this issue was not fully addressed, so any positive cellular drug response could be obscured by cell heterogeneity. Here, we address this issue by putting forward the same-single-cell analysis (SASCA), and we report a study of the drug efflux modulation of single multidrug resistant leukemia cells. We have demonstrated that the dynamic drug efflux in a single cell as modulated by a common Pgp modulator (i.e., verapamil) can be verified using SASCA, but not DISCA. To apply this approach to seek new beneficial MDR modulators from Chinese traditional medicine, the MDR modulation effects of two herbal ingredients with anticancer properties (isoliquiritigenin and sodium artesunate) were studied as well.

EXPERIMENTAL SECTION

Chip Design. The layout of the microfluidic chip, as shown in Figure 1a, consists of 3 channels, 3 reservoirs and 1 chamber containing a cell retention structure. Reservoir 1 is the cell inlet, reservoir 2 is the waste outlet, and reservoir 3 is used for reagent delivery. The glass chip was fabricated by Canadian Microelectronic Corporation (CMC, Protolyne Chip) by the standard microfabrication procedure. The etch depth was 20 μm, while the reservoirs were 600 μm deep and 2 mm in diameter. An image of the microchip filled with a red food dye is shown in Figure 1b.

Reagents. Daunorubicin (DNR), verapamil (VER), isoliquiritigenin (IQ), fluorescein diacetate, vinblastine and penicillin were obtained from Sigma-Aldrich (St. Louis, MO). Sodium artesunate (ART) was kindly provided by Dr. Thomas Efferth (German Cancer Research Centre, Heidelberg, Germany). IQ and ART were dissolved in DMSO (Sigma) to make stock solutions. Hanks' balanced salt solution (HBSS) was from Invitrogen Corp. (Grand Island, NY). α-MEM medium was purchased from Gibco (Grand

(23) Klauke, N.; Smith, G. L.; Cooper, J. *Biophys. J.* **2003**, *85*, 1766–1774.
(24) Shelby, J. P.; White, J.; Ganesan, K.; Rathod, P. K.; Chiu, D. T. *Proc. Natl. Acad. Sci. U.S.A.* **2003**, *100*, 14618–14622.
(25) Sims, C. E.; Allbritton, N. L. *Lab Chip* **2007**, *7*, 423–440.
(26) Carlo, D. D.; Lee, L. P. *Anal. Chem.* **2006**, *78*, 7918–7925.
(27) Teruel, M. N.; Meyer, T. *Science* **2002**, *295*, 1910–1912.
(28) Wheeler, A. R.; Throndset, W. R.; Whelan, R. J.; Leach, A. M.; Zare, R. N.; Liao, Y. H.; Farrell, K.; Manger, I. D.; Daridon, A. *Anal. Chem.* **2003**, *75*, 3581–3586.
(29) Negulescu, P. A.; Shastri, N.; Cahalan, M. D. *Proc. Natl. Acad. Sci. U.S.A.* **1994**, *91*, 2873–2877.
(30) Kennedy, R. T.; Oates, M. D.; Cooper, B. R.; Nicherson, B.; Jorgenson, J. W. *Science* **1989**, *246*, 57–63.
(31) Jin, W.; Li, X.; Gao, N. *Anal. Chem.* **2003**, *75*, 3859–3864.
(32) Li, P. C. H.; de Camprieu, L.; Cai, J.; Sangar, M. *Lab Chip* **2004**, *4*, 174–180.

Island, NY), and fetal bovine serum (FBS) was obtained from ATCC (Manassas, VA). All reagents were of analytical grade.

Cell Culture. The human wild-type leukemic cell line CCRF-CEM (CEM/wt, drug-sensitive) and its multidrug-resistant vinblastine-selected subline (CEM/VLB0.05) were maintained in α-MEM medium supplemented with 10% fetal bovine serum and 50 U/mL penicillin in a 5% CO_2 atmosphere at 37 °C. The cells were passaged twice a week, with the drug resistance of the CEM/VLB cell line stabilized by 0.05 mg/mL vinblastine for 4 days every 6 weeks.[10]

Single-Cell Selection and Retention. The single CEM cell was selected and retained as shown in Figure S-1 in the Supporting Information. Briefly, after a cell suspension (~0.1×10^6 cells/mL) was introduced into reservoir 1 (see Figure 1a for its location), the cells flowed from the right to the left (see Figure S-1a in the Supporting Information). By adjusting the liquid levels of reservoirs 1 and 2, a desired cell was slowed down near the entrance of the cell retention structure (Figures S-1b in the Supporting Information). Then, a flow at the central reagent channel was induced to push the cell into the retention structure (Figures S-1c in the Supporting Information). The cell was allowed to settle further for ~15 min (900 s) before the fluorescence measurement started. Figure 1c shows the image of a single CEM/VLB cell retained in the cell retention structure. The cell was alive after retention, which could be confirmed using fluorescein diacetate, as shown in the inset of Figure 1c.

On-Chip Drug Efflux Study on Single Cells. An optical detection system consisting of an inverted microscope (TE300, Nikon, Mississauga, ON, Canada) was employed for simultaneous fluorescence measurement and bright-field observation (see Figure S-2 in the Supporting Information), as previously described.[17,33] Using a dichroic filter (620 nm), only red light for cell observation entered the video camera; whereas the orange fluorescent emission (λ_{em} = 585 nm) under the blue excitation (λ_{ex} = 470 nm) was transmitted to the PMT through a detection aperture. The chip was translated back and forth so that the detection aperture window observed the cell or its surrounding region in turn. When the cell was in or out of the detection aperture, the cellular fluorescence or background signal was measured, respectively. We measured the fluorescence of the drug daunorubicin because of its inherent fluorescence and its being a substrate of the MDR1 transporter,[6,34] instead of measuring rhodamine 123, which could be used as a substrate, as reported in a previous efflux study.[35]

In the different-single-cell analysis, after one CEM cell (e.g., cell 1) was selected and retained in the cell retention structure, the cell media in all the reservoirs were removed, and then reservoir 3 was topped up with daunorubicin (35 μM) and left for ~1000 s. Fluorescent measurement was started to observe the DNR accumulation in the cell. The small space in front of the cell retention structure allowed an essentially instantaneous replacement of the cell medium around the cell by the DNR solution. After the accumulation phase, the solutions in all reservoirs were removed, and the cell medium (i.e., no DNR) was added to reservoir 3 and left for ~1800 s. This was to wash away the extracellular DNR, and at the same time, the cellular fluorescent intensity during drug efflux in cell medium was measured for ~1800 s. Then, the procedure was repeated on a second retained cell (e.g., cell 2). Briefly, it was treated with 35 μM DNR for ~1000 s, and drug efflux was conducted in cell medium containing a MDR inhibitor candidate compound (i.e., VER, IQ or ART) for ~1800 s. The two sets of fluorescent intensity curves were depicted in the schematics shown in Figure 2a. Comparison of the 2 efflux curves (Ed1 vs Ed2) were made subsequently, see Figure 2a inset.

In the same-single-cell analysis, only one retained cell (e.g., cell 3) was used. It was first treated with 35 μM DNR for ~1000 s in the drug accumulation step. Thereafter, drug efflux was conducted in cell medium alone for ~1800 s (control experiment). Then, the same cell was treated a second time with 35 μM DNR for ~1000 s, and a second drug efflux was conducted in cell medium containing a MDR inhibitor candidate compound (i.e., VER, IQ or ART) for ~1800 s. The fluorescent intensity curves were depicted in the schematics shown in Figure 2b. Comparison of the 2 efflux curves (Es3 vs Es3′) was then made, see Figure 2b inset. The time needed to complete this procedure was ~115 min as described in Table S-1 in the Supporting Information.

Flow Cytometry. Flow cytometry was performed using a fluorescence-activated cell sorter (FACS, Becton-Dickinson FACScalibur, San Jose, CA) to confirm the microfluidic on-chip single-cell analysis results. A previously reported procedure was followed.[9] Briefly, an aliquot (750 μL) of the cells (300,000 cells/mL) in the cell culture medium was transferred to a plastic tube containing 750 μL of incubation medium with DNR (35 μM). Drug accumulation was conducted at 23 °C for 30 min in the dark. After centrifugation (200*g* for 5 min) and removal of the supernatant, the cells were reincubated in the cell medium alone (i.e., without DNR) at 23 °C for an additional 30 min (the efflux phase). After a second centrifugation (200*g* for 5 min), the supernatant was removed. Cold HBSS was then added to each tube to quench the efflux. The cell suspension was transferred to a FACS tube, and was stored on ice (less than 15 min) before analysis. Fluorescence intensity (excitation at 488 nm, emission at 570/30 nm) was collected and displayed as single-parameter histograms, based on acquisition of data from 10,000 cells. The procedure was repeated for conducting efflux study of the cells in the presence of a MDR modulator compound (e.g., VER, IQ and ART). The time needed to complete this procedure was ~149 min. as described in Table S-1 in the Supporting Information.

RESULTS AND DISCUSSION

Different-Single-Cell Analysis (DISCA) for Drug Efflux Study in a Microchip. In this drug efflux study, to identify whether a MDR modulator compound (e.g., verapamil) has the MDR reversal effect or not, DNR efflux was conducted on a CEM/VLB cell (test cell) in the presence of the modulator compound and then on another cell (control cell) in the absence of the compound. As described in Figure 2a inset, the 2 efflux curves (Ed1 vs Ed2) obtained from 2 different cells were compared.

In the results shown in Figure 3a, we observe the typical efflux curves of different single drug-resistant cells (CEM/VLB) in various DNR-free solutions such as verapamil, IQ, and the cell medium alone. It was observed that the DNR efflux was fast

(33) Peng, X. Y.; Li, P. C. H. *Lab Chip* **2005**, *5*, 1298–1302.
(34) Fu, D.; Roufogalis, B. D. *Am. J. Physiol. Cell Physiol.* **2007**, *292*, c1543–c1552.
(35) Mazzanti, R.; Gatmaitan, Z.; Croop, J. M.; Shu, H.; Arias, I. M. *J. Cell Pharmacol.* **1990**, *1*, 50–56.

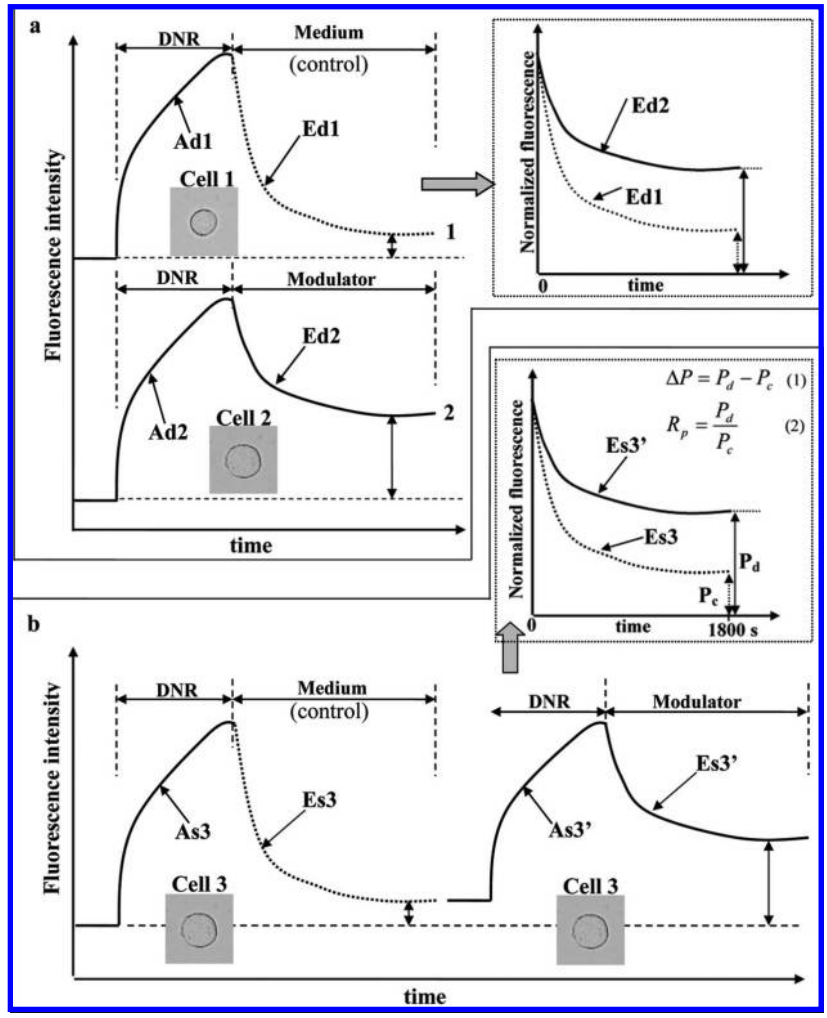

Figure 2. The schematic illustration of DISCA and SASCA for single-cell MDR efflux study. (a) In DISCA, two different cycles of accumulation and efflux occur on two different cells, namely cell 1 (Ad1 and Ed1), and cell 2 (Ad2 and Ed2). MDR modulation is evaluated by comparing the normalized fluorescent intensity of Ed2 and that of Ed1 (different cell control) shown in the inset. (b) In SASCA, one and the same cell was used in the 2 cycles of drug accumulation (As3, As3′) and efflux (Es3, Es3′). MDR modulation is evaluated by comparing the normalized fluorescent intensity of Es3′ with that of Es3 (same cell control) shown in the inset. P_d and P_c are the DNR retention percentages in the MDR modulator solution, and in the medium alone (control) at efflux time of 1800 s, respectively. They are determined by dividing the cell fluorescent intensity at efflux time of 1800 s, with the maximum fluorescent intensity before the efflux phase.

initially (i.e., 0−500 s). After that, the efflux rate slowed down and the cellular fluorescence did not change significantly. In addition, less DNR was retained (i.e., 0.2−0.4 or 20−40%) when the efflux was conducted in the medium (the efflux-in-medium curve) as compared to the efflux conducted in verapamil (the efflux-in-verapamil curve). This observation is consistent with the notion that verapamil interferes with the drug efflux process by binding to the Pgp efflux pump, thus resulting in MDR reversal and more DNR retention.[9,36] We also studied the MDR effect of another compound, IQ, an ingredient of the traditional Chinese herb licorice reported to have antitumor effects on human gastric cancer,[37] prostate cancer[38] and hepatoma.[39] However, no obvious inhibition effect of IQ on DNR efflux was observed as the efflux-in-IQ curves were similar to the efflux-in-medium curves (see Figure 3a).

What Figure 3a shows are just the typical curves of DNR efflux among other results obtained from multiple individual cells. The typical curves represent the cluster of the curves for most cells, as opposite to some outliers, see Figure 3b−d (see also Figure S-3 in the Supporting Information). Even in the same cluster, some cellular variations were still observed. For instance, Figure 3b shows the variations in the cluster of the drug-resistant cell line (CEM/VLB) and that of the CEM wild-type cell line (CEM/wt). Although it can be comfortably inferred that there is a lower drug retention in the CEM/VLB cells than in the CEM/wt cells, which was attributed to the overexpressed Pgp pumps in the CEM/VLB cells,[4] there are still a lot of variations observed in both clusters. It can be observed that some curves of CEM/VLB cells are even

(36) Akiyama, S. I.; Cornwell, M. M.; Kuwano, M.; Pastan, I.; Gottesman, M. M. *Mol. Pharmacol.* **1988**, *33*, 144–147.
(37) Ma, J.; Fu, N. Y.; Pang, D. B.; Wu, W. Y.; Xu, A. L. *Planta Med.* **2001**, *67*, 754–757.
(38) Kanazawa, M.; Satomi, Y.; Mizutani, Y.; Ukimura, O.; Kawauchi, A.; Sakai, T.; Baba, M.; Okuyama, T.; Nishino, H.; Miki, T. *Eur. Urol.* **2003**, *43*, 580–586.
(39) Hsu, Y.; Kuo, P.; Lin, C. *Life Sci.* **2005**, *77*, 279–292.

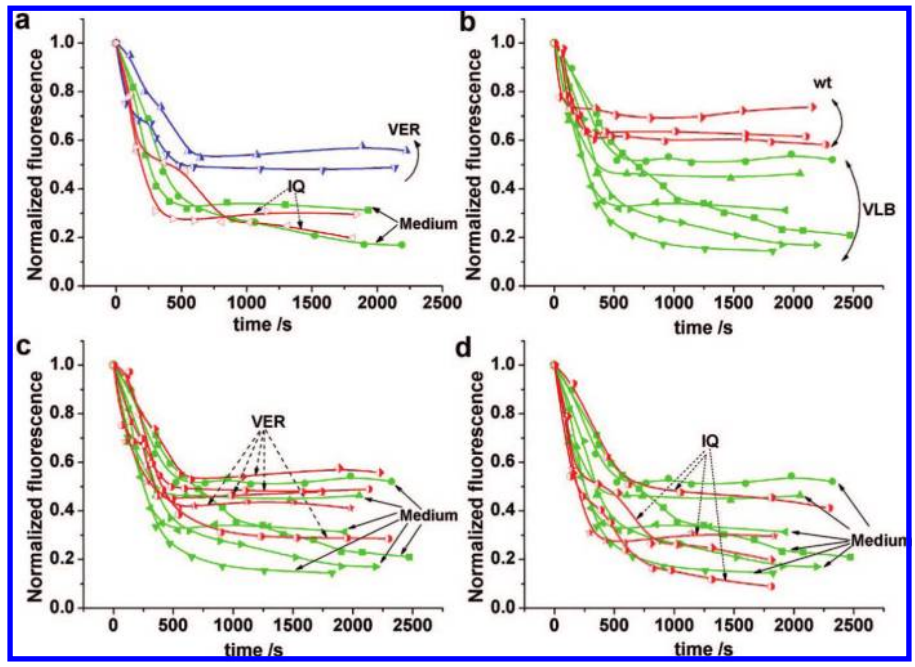

Figure 3. Modulation of DNR efflux by VER and IQ studied by DISCA in a microchip. (a) The typical curves of DNR efflux of CEM/VLB cells in the medium (green, solid symbols), in 50 μM verapamil (blue, half-filled symbols) and in 100 μM IQ (red, hollow symbols). (b) Comparison of DNR efflux in medium between CEM/wt (red, half-filled symbols) and CEM/VLB (green, solid symbols) cells. (c) The effect of verapamil (red, half-filled symbols) on the DNR efflux in CEM/VLB cells. (d) The effect of IQ (red, half-filled symbols) on the DNR efflux in CEM/VLB cells. The efflux curves are separately shown in Figure S-3a (wt-medium), S-3b (VLB-medium), S-3c (VLB-VER) and S-3d (VLB-IQ) in the Supporting Information.

close to those of the CEM/wt cells, indicating that some CEM/VLB cells have more drug retention due to less Pgp pump activities.

In the cases of drug efflux in verapamil and in IQ, the MDR reversal effects due to these compounds cannot be concluded due to the enormous cell variations in the efflux-in-verapamil cluster, and the efflux-in-IQ cluster, as shown in Figure 3c and 3d, respectively. Although it is well-known that verapamil could inhibit the MDR efflux and result in more drug retention,[9,36] this positive effect of MDR reversal cannot be verified in Figure 3c as some efflux-in-verapamil curves are mixed with the efflux-in-medium curves. Since the effect of IQ on MDR reversal is unknown, it is difficult to draw any conclusion when we examine Figure 3d. Under such situations, we chose to select the typical curves in each case (shown in Figure 3a) from many single-cell experiments, and tentatively conclude that there is a MDR reversal effect by verapamil, but not IQ.

Even though more single-cell experiments could help the data interpretation, we believe that this still cannot clarify the situation because one drawback of using DISCA for the MDR efflux study is the inevitable variations in cellular properties, such as the MDR activities, among different cells. In a worse case scenario, if the control cell has a lower drug efflux ability (i.e., the highest efflux-in-medium curve in Figure 3c), and the test cell has a greater drug efflux ability (e.g., the lowest efflux-in-verapamil curve in Figure 3c), the MDR reversal effect of the candidate will not be obvious, leading to a wrong conclusion.

Same-Single-Cell Analysis (SASCA) for Drug Efflux Study in a Microfluidic Chip. In order to minimize these cellular variations, we introduce SASCA for drug efflux study in which the same cell is employed as the control cell as well as the test cell. This demands the single cell to be retained long enough for the course of the drug efflux study, achievable by the cell retention ability of the microfluidic chip. The schematic diagram in Figure 2b shows the concept of the SASCA, in which 2 cycles of DNR accumulation and efflux steps are conducted on the same single cell (i.e. cell 3). As described in Figure 2, the 2 efflux curves (Es3 vs Es3′) obtained from one and the same cell were compared in SASCA, but the 2 efflux curves (Ed1 vs Ed2) from 2 different cells were compared in DISCA.

Figure 4a shows that there is a greater DNR retention when the cell efflux was conducted in the presence of verapamil by SASCA, and so it is clear that verapamil has reversed the DNR efflux process. More SASCA experiments show the same result of MDR reversal by the modulator, verapamil (see Table 1). This conclusion could not have been possible if the DISCA method had been used, see Figure 3c in which the efflux-in-verapamil and efflux-in-medium curves were not distinctly separated due to the cellular differences in MDR abilities.

To confirm the effect of verapamil using the conventional technique, flow cytometry was performed, resulting in the histograms shown in Figure 4b. It is found that the fluorescent intensity (plotted as the *x*-axis), which indicates the intracellular DNR retention, is greater when the drug efflux study is conducted in verapamil than in the cell medium alone, corroborating the microfluidic results. In the flow cytometry experiment, during the drug accumulation and efflux procedures (a total of 60 min.) before data collection, no cellular information is collected. But, in SASCA, the full profile of the drug transport from the same single cell is recorded even during drug accumulation and efflux. In addition, this approach has provided information about the cell morphology, which can be seen in the cell images in the Figure 4a inset, showing little cell shape changes, and nonstaining by trypan blue. This suggested that the cell was still viable, indicating that not

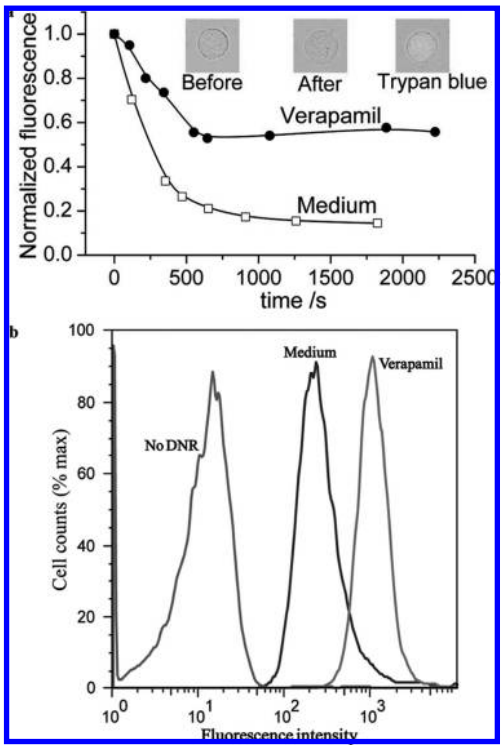

Figure 4. Modulation of verapamil (50 μM) on DNR efflux of CEM/VLB cells studied by SASCA and confirmed by flow cytometry. (a) SASCA for the study of the effect of MDR reversal by verapamil on one and the same CEM/VLB cell. The fluorescence intensities of DNR efflux in medium and in verapamil have been normalized for easy comparison. The inset images the cell morphologies before and after the experiment, and after trypan blue treatment. (b) Flow cytometry study of the modulation of DNR efflux in CEM/VLB cells by verapamil. The histograms represent the normalized percentage of cell counts plotted against the fluorescent intensity expressed as log relative fluorescence. The histograms depict, from left to right, the cells without DNR accumulation, the cells with DNR efflux in medium alone and the cells with DNR efflux in verapamil.

only the drug-resistant cell was not killed by DNR after substantial drug efflux but also the microfluidic method was robust for long-term cell measurement. The cell images could also be useful in documentation and data interpretation of the MDR reversal response. In addition, SASCA can comfortably select one cell from a small cell population of ~100, but flow cytometry requires ~100,000 cells to achieve high yield in data collection. A full comparison between flow cytometry and SASCA, in terms of experimental time, information content, throughput and automation, is tabulated in Table S-1 in the Supporting Information.

In a similar manner, the effect of IQ on MDR efflux was studied. It is now clear in Figure 5a that IQ did not result in a greater DNR retention, so IQ was ruled out as a MDR modulator candidate. Again, the use of the same cell as both the control and test cell in SASCA rules out the variations among different cells and assists in a conclusive data interpretation. More experiments on IQ (see Table 1) were repeated, and the same observation of no MDR reversal by IQ was achieved. The microchip data are also consistent with the histograms obtained by conventional flow cytometry (Figure 5b), which shows that CEM/VLB cells have a similar DNR retention in IQ as in medium alone, while DNR retention in CEM/wt cells is greater than that of the CEM/VLB cells. Similar to the verapamil experiment, the flow cytometry data did not give more information than SASCA in the conclusion of the IQ effect, though the histograms provide valuable information in cell distribution, which may be important in some applications such as the cell-cycle study.

To quantitatively evaluate the MDR modulations or MDR reversal effects of various drug candidates, we define 2 parameters, ΔP and R_p, as follows:

$$\Delta P = P_d - P_c \quad (1)$$

$$R_p = P_d / P_c \quad (2)$$

where P_d and P_c are the DNR retention percentages in the MDR modulator solution and in the medium alone (control), respectively, see Figure 2b inset. In flow cytometry, the fluorescence geometric mean ratio, G_p, is used, as defined in eq 3.[9,11]

$$G_p = G_d / G_c \quad (3)$$

where G_d and G_c are the fluorescence geometric means in the MDR modulator solution and in the medium (control), respectively. But the highest fluorescence geometric mean of the cells just after accumulation, denoted as G_a, is not normally measured.

Three different experiments of 50 μM verapamil by SASCA show that the highest values of ΔP and R_p are 41.3 and 3.87, respectively (Table 1), indicating that cell 3 would have the greatest MDR reversal effect. This has demonstrated the capability of SASCA to evaluate the different cellular abilities in response to drug efflux modulation. To compare with the flow cytometry data, the average values were used, and the average ΔP and R_p for verapamil (50 μM) are 21 ± 17% and 2.3 ± 1.4 (n = 3), respectively (Table 1). The values of ΔP and R_p for IQ (100 μM) are similarly compared, and they are −1.1 ± 5.1% and 0.88 ± 0.25 (n = 3), respectively. The R_p values (2.3 ± 1.4 and 0.88 ± 0.25) for verapamil and IQ are similar to the G_p values (3.83 ± 0.86 and 0.72 ± 0.21) obtained from flow cytometry data. The difference in R_p and G_p values may result from the differences between these two measurement methods, and the amount of tested cells, but this does not affect the conclusion of MDR modulation in both cases. Although R_p is defined for comparison with the results obtained from the flow cytometry method (e.g., G_p), we believe ΔP should be used in evaluating the drug candidate's MDR reversal effect in SASCA since the P_d and P_c values have already been normalized into the percentages. Moreover, R_p may be substantially affected by the denominator (P_c), especially when the value of P_c is very small.

The MDR modulation effect of another herbal ingredient sodium artesunate (ART) was also studied. ART derived from "Qinghao" was first discovered as an antimalarial drug,[40] and subsequently found to have anticancer property.[41] Figure 6 shows that the DNR efflux is reversed in the presence of ART, as compared with the efflux in the cell medium (medium 1, before ART). In order to confirm this finding, a second efflux step in the medium (medium 2) was conducted after the MDR reversal by ART. It was found that the efflux-in-medium curve in the second

(40) Dai, L.; Chen, Y. *Chemtracts* **1999**, *12*, 687–694.
(41) Wang, Q.; Wu, L.; Zhao, Y.; Zhang, X. L.; Wang, N. *Acta Pharm. Sin.* **2002**, *37*, 477–478.

Table 1. DNR Efflux in CEM/VLB Cells as Modulated by IQ, VER and ART Using SASCA[a]

	verapamil (VER)			isoliquiritigenin (IQ)			artesunate (ART)			
	cell 1	cell 2	cell 3	cell 4	cell 5	cell 6	cell 7	cell 8	cell 9	cell 10
P_d (%)	42.2	28.8	55.7	29.6	45.3	8.8	19.3	35.7	68.8	66.1
P_c (%)	31.7	17.2	14.4	31.7	40.8	14.4	14.9	10.8	47.6	38.0
ΔP (%)	10.5	11.6	41.3	−2.1	4.5	−5.6	4.4	24.9	21.2	28.1
average ΔP (%)		21 ± 17			−1.1 ± 5.1			19.7 ± 10.6		
$R_p = P_d/P_c$	1.33	1.67	3.87	0.93	1.11	0.61	1.30	3.31	1.45	1.74
average R_p		2.3 ± 1.4			0.88 ± 0.25			1.95 ± 0.92		
G_p		3.83 ± 0.86			0.72 ± 0.21			1.39		

[a] See eqs 1 to 3 for the definitions of P_d, P_c, ΔP, R_p, and G_p. ΔP gives the DNR retention percentage that the drug candidate can reverse. The bigger is ΔP, the greater is the drug's MDR reversal. On the other hand, a negative ΔP value means that the drug candidate potentiates the drug efflux, resulting in less drug retention. R_p is defined for comparison with the data obtained from the flow cytometry method (i.e., G_p). The higher is the R_p value, the greater is the MDR inhibition effect; $R_p = 1$ means that the drug candidate does not have any MDR modulation effect. If R_p is less than 1, it means the drug candidate potentiates the drug efflux.

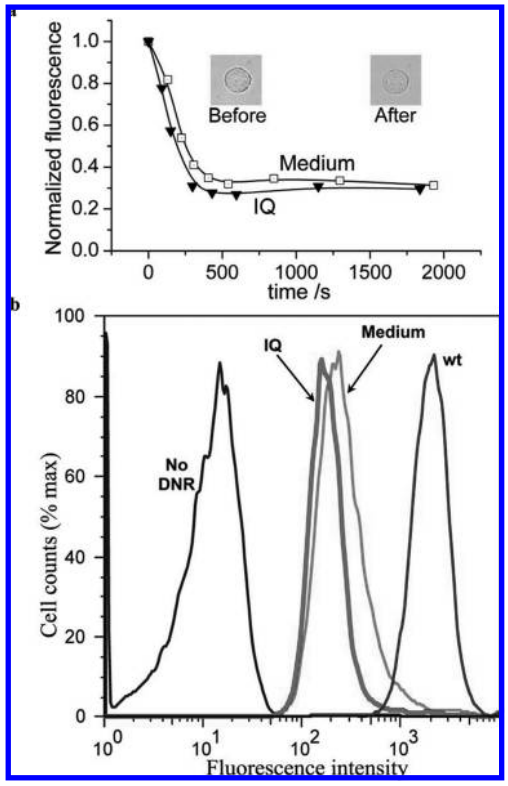

Figure 5. Effect of IQ on DNR efflux of CEM/VLB cells studied by SASCA and confirmed by flow cytometry. (a) Effect of IQ (100 μM) on MDR reversal studied on one and the same CEM/VLB cell by SASCA. Other conditions are the same as in Figure 4a. (b) Flow cytometry study of DNR efflux in CEM cells as treated by IQ. The histograms represent, from left to right, the CEM/VLB cells without DNR accumulation, the CEM/VLB cells with DNR efflux in IQ (100 μM), the CEM/VLB cells with efflux in medium alone, and the CEM/wt cells with DNR efflux in medium alone. Others conditions for flow cytometry are the same as in Figure 4b.

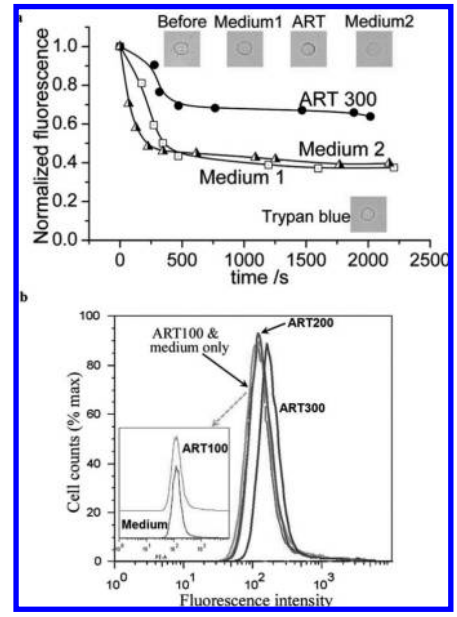

Figure 6. Modulation of artesunate on DNR efflux of CEM/VLB cells studied by SASCA and confirmed by flow cytometry. (a) Effect of MDR reversal by ART (300 μg/mL) studied by SASCA on one and the same CEM/VLB cell in a microfluidic chip. A second efflux in medium (medium 2) confirmed that the effect of 300 μg/mL ART (ART300) was genuine after the first efflux in medium (medium 1). Both efflux steps in medium alone were used as control experiments. Other conditions are the same as in Figure 4a. (b) Flow cytometry study of the effect of artesunate (100, 200, 300 μg/mL) on DNR efflux in CEM/VLB cells. The histograms from the medium alone and 100 μg/mL artesunate are offset vertically and shown in the inset since these two peaks are very close to each other. Others conditions for flow cytometry are the same as in Figure 4b.

time was consistent with that in the first one, confirming the finding that the MDR modulation effect of ART was genuine. More same-single-cell experiments also confirmed the effect of artesunate (300 μg/mL) on MDR efflux, as shown by the mean values of ΔP and R_p, which are 19.7 ± 10.6% and 1.95 ± 0.92, respectively (see Table 1). It has been reported that ART (60 μg/mL) significantly increased DNR accumulation in the MRP1-expressing cells, but not observed in the MDR1-expressing CEM cell line.[10] In our hands, it was discovered that when ART was more concentrated than 200 μg/mL, it produced a beneficial MDR inhibition effect, consistent with the flow cytometry data (Figure 6b). But no inhibition effect on MDR efflux was observed in lower concentration of ART (100 μg/mL).

CONCLUSION

The same-single-cell analysis conducted in a microfluidic chip has demonstrated the advantages in identifying MDR modulators, and in quantifying the MDR reversal effect of drug candidates based on the defined parameter of ΔP. It has been demonstrated that SASCA is superior to DISCA by ruling out the difference in MDR activities among different cells and presenting a conclusive

result about the effect of MDR modulators by using the same cell as both the test and the control cell. SASCA is also compared with the conventional flow cytometry method in the study of MDR modulator candidates. The time needed to conduct SASCA is shorter than in flow cytometry, and the microfluidic operation will become less tedious after automation in cell manipulation and fluorescent data collection. In the research communities, the microfluidic method SASCA can provide time-dependent drug transport kinetics and cell morphological information, and only a small number of cells is needed to confirm the findings. Therefore, this technique may have significant potential for investigating drug resistance in minor cell subpopulations (e.g., cancer "stem" cells) that may be the key determinant of clinical response to chemotherapy, and seeking effective chemotherapy drugs for patients in clinic as well. In addition, this microchip-based method, SASCA, is envisioned for clinical use as a prognostic method, e.g. to check the MDR profile and drug responses so as to look for personalized drugs before patient treatment starts.

ACKNOWLEDGMENT

Financial support from Natural Science and Engineering Research Council of Canada (Idea-to-Innovation) and Canadian Microelectronic Corporation (Protolyne) is acknowledged. We are also grateful to Dr. Thomas Efferth (German Cancer Research Centre, Heidelberg) for providing sodium artesunate, Dr. Jamie Scott for the use of the FACS instrument, Matina Mai for acquiring the flow cytometry data, and Barbara Schmidt for advice in cell culture.

SUPPORTING INFORMATION AVAILABLE

Additional information as noted in text. This material is available free of charge via the Internet at http://pubs.acs.org.

Received for review February 1, 2008. Accepted March 21, 2008.

AC800231K